HHS Public Access

Author manuscript

Cell. Author manuscript; available in PMC 2017 February 11.

Published in final edited form as:

Cell. 2016 February 11; 164(4): 695–709. doi:10.1016/j.cell.2015.12.036.

Actin dynamics regulates dendritic cell-mediated transfer of HIV-1 to T cells

Mickaël M. Ménager[1,3] and **Dan R. Littman**[1,2,3]

[1]Molecular Pathogenesis Program, The Kimmel Center for Biology and Medicine of the Skirball Institute, New York University School of Medicine, New York, NY 10016, USA

[2]The Howard Hughes Medical Institute

SUMMARY

Whereas human dendritic cells (DCs) are largely resistant to productive infection with HIV-1, they have a unique ability to take up the virus and transmit it efficiently to T lymphocytes through a process of *trans-infection* or *trans-enhancement*. To elucidate the molecular and cell biological mechanism for *trans-enhancement*, we performed an shRNA screen of several hundred genes involved in organelle and membrane trafficking in immature human monocyte-derived dendritic cells (MDDCs). We identified TSPAN7 and DNM2, which control actin nucleation and stabilization, as having important and distinct roles in limiting HIV-1 endocytosis and in maintaining virus particles on dendrites, which is required for efficient transfer to T lymphocytes. Further characterization of this process may provide insights not only into the role of DCs in transmission and dissemination of HIV-1, but more broadly into mechanisms controlling capture and internalization of pathogens.

INTRODUCTION

Despite major progress in unraveling the mechanism of the HIV replication cycle in human T lymphocytes, the role of cells involved in the innate response to HIV and other retroviruses is only now receiving growing attention. Dendritic cells (DCs) serve a key function in host defense, linking innate detection of microbes to activation of pathogen-specific adaptive immune responses (Banchereau et al., 2000). DCs express cell surface receptors for HIV-1 entry, but undergo very limited productive infection as a result of host cell restriction factors (Wu and KewalRamani, 2006). DCs do, however, facilitate infection of co-cultured T-helper cells through a process of *trans*-enhancement (Cameron et al., 1992; Geijtenbeek et al., 2000). A cell-intrinsic sensor for HIV-1, cGAS, has the potential to activate the type I interferon response to reverse-transcribed viral DNA in DCs, but is not

[3]To whom correspondence should be addressed: dan.littman@med.nyu.edu, mickael.menager@med.nyu.edu.

AUTHOR CONTRIBUTIONS

M.M.M designed, performed and analyzed all the experiments. D.R.L. supervised the research and participated in experimental design. M.M.M and D.R.L. wrote the manuscript.

typically engaged owing to a block in reverse transcription mediated by the host dNTP hydrolase SAMHD1 (Gao et al., 2013; Laguette et al., 2011; Lahaye et al., 2013; Manel et al., 2010). The virus appears to have evolved to avoid infecting these cells, and it has been proposed that it instead exploits DCs to facilitate rapid infection of a large pool of T cells and, perhaps, to reside in non-replicating reservoirs within DCs (Wu and KewalRamani, 2006).

Trans-enhancement is defined as the capacity of dendritic cells to augment infection of T cells with a minimal HIV inoculum (Cameron et al., 1992; Geijtenbeek et al., 2000). Binding of the HIV envelope glycoprotein to mannose receptors has been implicated in trans-enhancement, although the C-type lectin DC-SIGN is not absolutely required (Boggiano et al., 2007; Geijtenbeek et al., 2000; Kwon et al., 2002). Recently, SIGLEC-1 (CD169) was described as an interferon-inducible receptor for HIV-1 transfer from LPS-matured DCs to T cells (Izquierdo-Useros et al., 2012).

Trans-enhancement was originally thought to involve classical endocytosis (Kwon et al., 2002), but it was later found that the internalized virus was still accessible to solvent (i.e. soluble CD4 could inactivate captured HIV) (Cavrois et al., 2007). This discrepancy was potentially reconciled by the observation that, in mature DCs, HIV-1 is internalized in a tetraspanin-rich compartment (containing CD81), called the "invaginated pocket", which is still accessible to solvent but is topologically distinct from the cell membrane (Yu et al., 2008).

To gain more insight into the mechanism of trans-enhancement, we performed an shRNA screen in immature human primary monocyte-derived DCs (MDDCs). We focused on several hundred genes involved in organelle and membrane trafficking to identify those that impact HIV-1 transfer, and identified and validated the function of tetraspanin 7 (TSPAN7) and dynamin 2 (DNM2). TSPAN7 is localized at the plasma membrane and has a critical role in neurite outgrowth (Bassani et al., 2012). The large GTPase DNM2 plays a key role in endocytosis (Ferguson and De Camilli, 2012) and is recruited to the neck of coated pits where it can assemble into a collar structure to mediate membrane fission. More recently, DNM2 was described as an important regulator at the interface between the membrane and the dynamic actin cytoskeleton, modulating actin nucleation and promoting the stability of the actin filament network (Ferguson and De Camilli, 2012; Gu et al., 2010; Lee and De Camilli, 2002; Orth et al., 2002). We show here that, during HIV-1 transfer from DCs, TSPAN7 and DNM2 control nucleation and cortical stabilization of actin, which limits HIV-1 endocytosis and maintains the virus on dendrites for efficient transfer to T lymphocytes.

RESULTS

RNA interference screen for genes involved in DC to T cell HIV transfer

To identify genes involved in the transfer of HIV-1 from DCs to T lymphocytes, we performed an shRNA screen, in human primary monocyte-derived dendritic cells (MDDCs), of 455 genes (4 or 5 shRNAs per gene) whose products are involved in organelle and membrane trafficking (Table S1). We used Vpx-containing SIV virus-like particles to

achieve highly efficient transduction of MDDCs with lentiviral vectors encoding the shRNAs. To assess the transfer of HIV-1 from MDDCs to T cells, we co-cultured transduced MDDCs at a ratio of 1:1 with autologous $CD4^+$ T cells activated with IL-2 and PHA (Figure 1A). The cultures were infected with a replication-competent CXCR4-tropic HIV-1 encoding GFP in place of Nef, and the proportion of infected GFP^+ $CD4^+$ T cells was assessed by flow cytometry after two days. There was no detectable replication of HIV-1 in MDDCs, and presence or absence of Nef had no impact on viral transfer from MDDCs to T cells (M.M.M unpublished data). Several controls were included for each donor: the PLK0.1 vector with a scrambled shRNA, empty vector, or transduction without vector, allowing assessment of nonspecific effects due to transduction and/or processing of shRNAs. The variation of transfer among the controls was lower than 5% on average, with a maximal variation never reaching more than 20% (Figure S1A and B). Among the targeted genes, we found a >30% decrease in HIV-1 transfer with at least 2 shRNAs for 43 genes and with one shRNA for 38 genes. Targeting of another 25 genes with at least 2 shRNAs per gene and of 28 genes with one shRNA increased transfer by at least 30% (Figure 1B and Table S1).

Among the hits for which we observed reduced HIV-1 transfer, there was enrichment for genes involved in actin nucleation (18 genes out of 81) and/or membrane protrusions (10 genes out of 81) (Figure S1C), including 4 out of the 7 subunits of the ARP2/3 complex. Direct regulators of this complex, including WASP and CDC42 (Rohatgi et al., 1999), also scored in the assay, as did CFL1, which promotes debranching of actin filaments and whose knockdown enhanced HIV-1 transfer (Martin et al., 2006). Proteins whose functions are mainly in formation and stabilization of cortical actin, including ARL13B (Casalou et al., 2014) and DNM2 (Ferguson and De Camilli, 2012; Gu et al., 2010; Lee and De Camilli, 2002; Menon et al., 2014; Orth et al., 2002), were similarly required for efficient HIV-1 transfer.

Hits that resulted in increased HIV-1 transfer were enriched for genes (24 out of 53) involved in several endocytic pathways (Figure S1D). These included genes involved in clathrin-mediated endocytosis (CME) such as those encoding clathrin heavy and light chain (CLTC, CLTB and CLTA), members of the clathrin-associated protein complexes AP-1 (AP1M1; AP1G1), AP-2 (AP2M1), and AP-4 (AP4M1), and myosin Va (MYO5A), an actin-based motor protein (Boettner et al., 2012; Doherty and McMahon, 2009). Genes encoding molecules involved in caveolin-mediated endocytosis included CAV3, CAV1 and FLOT1 (Glebov et al., 2006). Together, these results thus suggested roles for actin nucleation and endocytosis in enhancing or limiting HIV-1 transfer, respectively.

TSPAN7 is required for HIV-1 transfer and dendrite formation

Among the genes whose knockdown resulted in robust decrease in transfer (Figure 1B), TSPAN7 caught our attention, as it is a yet uncharacterized member of the tetraspanin family, for which several members (CD9, CD63, CD81, CD82) were reported to be involved in HIV-1 cell-to-cell transfer and/or trafficking (Garcia et al., 2005). We confirmed, using blood from multiple donors, a reproducible nearly 50% decrease of HIV-1 transfer using shRNA sequences targeting different regions of TSPAN7 as compared to scrambled shRNA (Figure 2A, B) (Bassani et al., 2012). The efficiency and the specificity of TSPAN7

knockdown were assessed by both quantitative PCR and immunoblot (Figure S2A, B). Additionally, TSPAN7 expression was induced during differentiation of MDDC from monocytes in the presence of GM-CSF and Il-4, and was correlated with appearance of dendrites (Figure S2C and M.M.M unpublished data).

By confocal microscopy, there was a marked change in dendritic cell morphology resulting from reduced TSPAN7 expression. Phalloidin staining revealed a loss of long and thin actin-rich membrane extensions, or dendrites, upon TSPAN7 knockdown (Figure 2C). Transmission and three-dimensional scanning electron microscopy (3D-SEM) analysis confirmed this effect and showed that a decrease in TSPAN7 expression shifted the balance from dendrites towards formation of short and large blebs of the plasma membrane (Figure 2D, E and Movie S1).

TSPAN7 prevents HIV-1 redistribution from dendrites to macropinosomes

To study localization of incoming HIV-1 particles by confocal microscopy, we exposed MDDC to replication-competent virus containing a Gag-internal green fluorescent protein (iGFP), as previously described (Hubner et al., 2007). Upon TSPAN7 shRNA knockdown, the loss of dendrites was accompanied by redistribution of HIV-1 particles from dendrites to cytosolic compartments, observed both by confocal (Figure 3A) and transmission electron microscopy (Figure 3B and C). By comparison, electron microscopy of control co-cultures revealed synaptic clefts with numerous HIV-1 particles in very close vicinity of dendrites, but HIV-1-loaded vesicles were abundant only in the infected T cells (Figure S2D). Aggregates of HIV-1 were present in large vesicles (between 0.3 and 1 μM) that also internalized dextran, a marker of macropinosome-like vesicles (94.8 ± 5% colocalization) (Wang et al., 2014) (Figure 3B, D and S2E), contained MHC class II and Rab7 (97.5 ± 2.9% and 93.38 ± 5% colocalization respectively), a marker for late endosomes, and were surrounded by the tetraspanin CD81(25.8 ± 9.3% colocalization), which is usually localized at the plasma membrane and in endosomes (Figure 3D). By electron microscopy, we were able to observe HIV-1 internalization through mechanisms resembling bleb retraction (Figure 3B, lower panel). There was no co-localization of HIV-1 aggregates with clathrin- or caveolin-positive vesicles (1.2 ± 0.9% and 1 ± 0.6% colocalization, respectively) or with markers of early endosomes (EEA1) and lysosomes (Lamp2) (6 ± 6.4% and 3.5 ± 5.3% colocalization, respectively) (Figure S2F and M.M.M unpublished data). Uptake by MDDCs of both dextran and HIV-1 particles was markedly enhanced upon knockdown of TSPAN7 (Figure 3E and S2G–J), consistent with increased macropinocytosis activity.

Together, these observations suggest that the decrease in HIV-1 transfer from MDDCs to T cells is linked to the loss of actin-rich dendrites and to an increase in virus uptake in macropinosomes.

Inhibition of ARP2/3 mimics TSPAN7 phenotypes

The ARP2/3 complex performs critical functions in formation of membrane protrusions and actin-rich structures, catalyzing actin filament nucleation required for assembly of actin filament networks (Goley and Welch, 2006). Treatment of MDDCs with CK666 and CK869, specific inhibitors of ARP2/3-mediated actin nucleation, reduced viral transfer

(Figure 4A, B and S3A) (Hetrick et al., 2013). The drugs had no effect on cell-free infection of T cells with HIV-1, supporting a specific role for actin nucleation in DC during viral transfer (Figure S3A). The decrease in transfer was accompanied by loss of actin-rich dendrites (Figure 4C, D), increased HIV-1 capture (Figure 4E, F), and increased virion uptake in macropinocytic-like vesicles (M.M.M unpublished data). There was a global increase of macropinocytosis-like endocytic processes upon inhibition of actin nucleation, with accumulation of dextran in MDDCs (Figure S3B–D). There was no synergistic or additive effect on HIV-1 transfer when ARP2/3 was inhibited in MDDCs treated with TSPAN7 shRNAs (Figure 4G, H).

Dendritic to T cell contact is required for HIV-1 trans-enhancement (McDonald et al., 2003). There was no change in the number of contacts between MDDCs and T cells upon inhibition of ARP2/3-mediated actin nucleation or TSPAN7 knockdown, as assessed by flow cytometry analysis of doublet formation (Figure S3E) and confocal microscopy analysis, in which conjugate formation was defined as contact between plasma membranes and enrichment of actin staining at the zone of contact (Figure S3F, G). However, the nature of the contacts was different, with a shift from dendrite-mediated contact to tight contact between plasma membranes (Figure S3F, G). No differences in surface expression of molecules previously implicated in DC-T cell interactions and HIV-1 transfer, including LFA-1, ICAM-1, SIGLEC-1, DC-SIGN, and DC-IR, were detected by flow cytometry analysis (M.M.M unpublished data). Thus, decreased HIV-1 transfer following inhibition of actin nucleation was most likely due to the loss of dendrites and an accumulation of HIV-1 in macropinocytic structures and not to reduced contact of MDDCs with T cells.

Requirement for DNM2 in HIV-1 transfer independent of dendrite formation

Dynamin 2 (DNM2), a strong hit in the shRNA screen (Figure 1 and 5A, B), has been implicated in nucleation and stabilization of actin networks (Gu et al., 2010; Lee and De Camilli, 2002; Menon et al., 2014; Orth et al., 2002). The specificity of DNM2 knockdown and function was validated by QPCR (Figure S4A) and by use of dynamin-specific inhibitors, Dynasore and Dyn V-32 (Yamada et al., 2009), that inhibited HIV-1 infection of T cells only when MDDCs were present in the co-culture (Figure 5C and S4B). After DNM2 knockdown, there was a 3-fold increase in HIV-1 capture (Figure 5D and S4C) and increased dextran internalization by MDDCs, similar to what was observed with TSPAN7 knockdown (Figure S4D, E). There was no difference in contacts between T cells and MDDCs (Figure S4F) or in surface expression of LFA-1, ICAM-1, SIGLEC-1, DC-IR and DC-SIGN (M.M.M unpublished data). HIV-1 was relocalized from dendrites to aggregates (Figure 5E, F) that were also positive for dextran uptake, Rab7, HLA-DP-DQ-DR and CD81 (Figure 5G) (89.4 ± 6%, 92.1 ± 3.4%, 95.1 ± 3.9% and 21.1 ± 5.1% colocalization, respectively), but differed from clathrin- or caveolae-associated vesicles, early endosomes and lysosomes (4.7 ± 1.4%, 8.9 ± 7.5%, 1.8 ± 1.6% and 1.4 ± 1.8% colocalization respectively) (Figure S4G). No synergy or additive effects were noticed when cells were treated with CK666, dynasore or a combination of both drugs, suggesting that they inhibit HIV-1 transfer through the same pathway (Figure 5H).

In contrast to inhibition of TSPAN7 expression, there was no noticeable reduction of actin-rich dendrites, as assessed by confocal microscopy, after blockade of DNM2 expression (Figure 5E). Electron microscopy revealed an unusual mix of dendrites and blebs at the surface of the dendritic cells (Figure S4H, left panel), with large vesicles (from 0.3 to 1 μM) that are likely macropinosomes containing HIV-1 particles (Figure S4H, right panel).

Although TSPAN7 and DNM2 differed in their requirement for dendrite formation and/or maintenance, there was disruption in the continuity of phalloidin staining beneath the plasma membrane when either molecule was knocked down, as shown by analysis and measurement of multiple Z-stack images (Figure S5). Disruption of the actin filaments following inhibition of TSPAN7 or DNM2 expression was associated with mis-localization of HIV-1 particles beyond the cortical region adjacent to the plasma membrane (Figure S5A). Together, these findings suggest that TSPAN7 and DNM2 are critical for establishment and/or maintenance of a stable cortical actin barrier that limits HIV-1 uptake by dendritic cells.

Inhibition of macropinocytosis can rescue HIV-1 transfer upon DNM2 knockdown in MDDCs

To assess the impact of HIV-1 internalization on its transfer to T cells, we treated MDDCs with inhibitors of the main endocytic pathways, before co-culturing them with HIV-1 and T cells. We established optimal conditions to inhibit clathrin- or caveolae-mediated endocytosis and macropinocytosis in MDDCs by respectively using chlorpromazine (CPZ), nystatin or rottlerin (Figure S6A, B) (Ivanov, 2008; Sarkar et al., 2005). We observed enhanced HIV-1 transfer with all inhibitors, but most prominently with rottlerin (Figure 6A and S6C). The increase in HIV-1 transfer was accompanied by decreased HIV-1 internalization, most marked in the presence of rottlerin, as monitored by flow cytometry after p24 intracellular staining (Figure 6B and C). Increased HIV-1 transfer was also observed in the presence of other drugs (IPA-3, 10 μM, NEIPA, 10 μM, Antimycin A1, 10 μM) that block macropinocytosis (Figure S6D, E).

These results suggested that uptake of HIV-1 by way of multiple pathways can reduce transfer to T cells. We found that, indeed, MDDCs can internalize small numbers of HIV-1 particles in vesicles containing either clathrin, caveolin or, more frequently, internalized fluorescently labeled dextran (26.9 ± 6.8%, 16.75 ± 5.61%, and 53.81 ± 12.5% colocalization, respectively) (Figure S6F). Macropinocytic events, depicted by plasma membrane ruffles folding back on HIV-1, were visible by electron microscopy (Figure S6G). HIV uptake by MDDCs thus appears to involve multiple mechanisms, although macropinocytosis is favored. The magnitude of this uptake differs from the much more prominent virion internalization observed almost exclusively in dextran-containing compartments following inhibition of TSPAN7 or DNM2 expression.

We next examined whether accumulation of HIV-1 in macropinosome-like vesicles, observed after TSPAN7 and DNM2 knockdown, contributes to decreasing HIV-1 transfer by lowering availability of HIV-1 at the plasma membrane. MDDCs in which TSPAN7 or DNM2 were knocked down were incubated with CPZ, rottlerin or nystatin and HIV-1 transfer to T cells was assessed. The endocytosis inhibitors had no apparent effect on

inhibition of transfer following TSPAN7 knockdown, despite their enhancement of transfer in control shRNA-treated MDDCs (Figure 6D, E). However, inhibition of macropinocytosis specifically restored HIV-1 transfer after knockdown of DNM2, to a level similar in magnitude to that observed in control shRNA-treated MDDCs (Figure 6D, E). Thus, inhibition of HIV-1 uptake by macropinocytosis overcomes dependency on DNM2, but not TSPAN7, for efficient HIV-1 transfer to T cells.

Inhibition of actomyosin contraction rescues dendrite formation and HIV-1 transfer

As inhibition of actin nucleation leads to the replacement of actin-rich dendrites with blebs, we next wondered what would be the impact on HIV-1 transfer if we blocked bleb formation. For this purpose, we inhibited non-muscle myosin II ATPase activity in MDDCs using the specific inhibitor blebbistatin (Straight et al., 2003). This inhibition resulted in a dose-dependent increase in HIV-1 transfer, following 2 h treatment of wild type MDDCs with the active enantiomer of blebbistatin (Figure 7A and S7A). Inhibiting actomyosin contractility also rescued HIV-1 transfer from MDDCs in which TSPAN7 or DNM2 had been knocked down or that were subsequently treated with CK666 or Dynasore (Figure 7A and S7A). We observed a very strong correlation (Pearson's correlation coefficient = 0.94) between the level of inhibition of HIV-1 transfer due to disruption of actin nucleation and the ability of blebbistatin to rescue and increase HIV-1 transfer (Figure S7B). Of note, treatment of T cells alone with either blebbistatin enantiomer had no effect on their infection with HIV-1 (Figure S7C).

The blebbistatin-mediated increase or rescue of HIV-1 transfer was linked to an impressive increase or restoration in formation of filopodia and actin-rich dendrites (Figure 7B, left and middle panels). This was accompanied by increased or restored localization of HIV-1 on actin-rich dendrites (quantified in Figure 7C). Inhibition of DNM2 function did not prevent the increase in filopodia and "extended" actin-rich dendrites, but limited the maintenance of HIV-1 on the "extended" dendrites (Figure 7B, right panel and 7C). By comparison, although inhibition of macropinocytosis with rottlerin attenuated HIV-1 internalization in multiple conditions (scramble, TSPAN7 or DNM2 shRNA knockdown), it did not enhance actin nucleation and formation of actin-rich dendrites (Figure 7B, C). Finally, active blebbistatin reduced the macropinocytosis-dependent HIV-1 and dextran internalization following TSPAN7 or DNM2 knockdown (Figure 7D and S7D).

In conclusion, inhibition of actomyosin contraction compensates for defective actin nucleation and cortical actin stability in MDDCs and thus facilitates HIV-1 localization on extracellular dendrites and concomitant viral transfer to T cells.

DISCUSSION

Although the phenomenon of trans-enhancement has been known for over two decades, studies to date have mainly focused on which DC receptors are involved and whether virions are internalized prior to being handed off to T cells. Actin-rich sheet-like membrane extensions dependent on Cdc42 were previously described as critical for HIV-1 transfer in immature MDDCs (Nikolic et al., 2011). Using a robust quantitative genetic screen, we were able to identify, with high confidence, that actin nucleation and an intact cortical actin

cytoskeleton are required to maintain HIV-1 association with dendrites and prevent engulfment of virus into macropinocytic vesicles. These results reinforce the growing consensus that HIV-1 is transmitted directly from the cell surface, rather than through an obligate endocytic pathway (Cavrois et al., 2008; Do et al., 2014; Yu et al., 2008)

TSPAN7 and regulation of actin nucleation

Tetraspanin family members are involved in multiple aspects of cell biology and physiology, including cell motility, signaling, morphology, neurite outgrowth, viral entry, and tumorigenesis (Charrin et al., 2014). In cultured hippocampal neurons, TSPAN7 is required for filopodia and dendritic spine formation and stabilization, a role that is consistent with the subcellular phenotypes associated with the characterized X-linked mental retardation pathology, due to mutations in *TSPAN7* (Bassani et al., 2012; Zemni et al., 2000). Even though TSPAN7 expression is not as high in MDDCs as in brain, its expression was induced during monocyte to dendritic cell differentiation, and correlated with the formation of dendrites. We found that inhibitors of the ARP2/3 complex phenocopied the TSPAN7 knockdown in MDDCs. As dendritic spine formation is dependent on actin nucleation, a role for TSPAN7 in regulating the actin cytoskeleton was proposed. Accordingly, the C-terminal tail of TSPAN7 binds the PDZ domain of PICK1 (Bassani et al., 2012), a molecule that interacts with ARP2/3 and F-actin filaments to inhibit actin nucleation (Rocca et al., 2008). Thus, in dendritic cells, TSPAN7 may sequester PICK1 to prevent its inhibition of ARP2/3. Another mode of action of TSPAN7 could be through interactions with phosphatidylinositide (PI) 4-kinase (PI4K) (Yauch and Hemler, 2000) and β1-integrin (Bassani et al., 2012; Berditchevski, 2001), which regulate the actin cytoskeleton through biosynthesis of phosphatidylinositol 4,5-bisphosphate and recruitment of ARP2/3 complex-interacting proteins to the vicinity of plasma membrane phosphoinositides (Berditchevski, 2001; Hilpela et al., 2004).

DNM2 and regulation of cortical actin

DNM2 is a large GTPase, which can self-assemble into higher order structures to promote endocytosis by stimulating the fission of budding vesicles upon GTP hydrolysis (Doherty and McMahon, 2009; Ferguson and De Camilli, 2012). DNM2 is also recognized as a regulator of the actin network and has been found co-localizing with actin-rich structures such as podosomes, actin comet tails, phagocytic cups, dynamic cortical ruffles and lamellipodiae (Ferguson and De Camilli, 2012; Gu et al., 2010). Within lamellipodiae, DNM2 regulates the spatiotemporal distribution of α-actinin and cortactin, actin-binding proteins that influence the actin network (Menon et al., 2014). DNM2 also binds directly to F-actin-filaments and aligns them into bundles and participates in the elongation of actin filaments by releasing the actin capping protein gelsolin (Gu et al., 2010). Interestingly, it has been reported that DNM2-depleted cells retain their capacity to form membrane protrusions even though there is a reduction in the dense network of branched cortical actin (Menon et al., 2014). This is consistent with our observation that, in MDDCs, there was retention of actin-rich dendrites despite the loss of a continuous barrier of cortical actin upon knockdown of DNM2.

Regulation of HIV-1 internalization by macropinocytosis

Our results show that, in MDDCs, extension of membrane protrusions and endocytosis are tightly linked and inversely correlated, based on their dependency on actin nucleation and cortical actin. Upon disruption of the cortical actin filament network, we observed a selective increase in macropinocytosis-mediated solute uptake and sequestration of HIV-1 particles in large intracellular vesicles, also enriched for MHC class II. Targeting of this pathway may thus improve presentation of HIV antigens to T cells, restricting viral dissemination.

The cortical actin network creates tension that inhibits endocytosis (Gauthier et al., 2012; Kaur et al., 2014), and debranching and subsequent actin remodeling and/or depolymerization are required for membrane bending and vesicle morphogenesis during endocytosis (Martin et al., 2006). Our results in MDDCs are consistent with such a role. A form of macropinocytosis that involves blebs, which are largely devoid of branched and polymerized actin, has been described for vaccinia virus, whose internalization has been linked to bleb retraction (Mercer and Helenius, 2008). TSPAN7 knockdown or CK666 treatment induced a switch from actin-rich protrusions to blebs. By inhibiting bleb formation using blebbistatin we demonstrated that increased internalization of HIV-1 occurs through bleb retraction, following disruption of actin nucleation. Treatment of MDDCs with blebbistatin also led to a marked increase in an “extended” network of actin-rich dendrites which were adorned with HIV-1 particles in a context of intact actin nucleation (Figure S7E). The concomitant increase in HIV-1 transfer reinforces the importance of viral maintenance on actin-rich dendrites in this process.

Bleb formation, which is driven by actomyosin contraction (Ridley, 2011), is antagonized in a dynamic and finely-regulated manner by Arp2/3 activity that controls the cellular actin cortex and cortical tension (Bergert et al., 2012). Growth cone collapse, that occurs in the absence of protrusive forces derived from actin nucleation, can be rescued by inhibition of contractile forces (actomyosin) produced by nonmuscle myosin II (Yang et al., 2012). Our data suggest that the same mechanism is utilized during formation of actin-rich dendrites in immature MDDCs (Figure S7E). Results with DNM2 knockdown, which reduced HIV-1 transfer and was reversed by inhibition of macropinocytosis, suggest that DNM2 functions independently of the ARP2/3 complex to control cortical actin stability (Figure S7E).

Dendritic cell function in HIV pathogenesis

Dendritic cells are likely the first cells to encounter and capture HIV-1 during viral transmission. By localizing to the surface of actin-rich filopodia-like structures, HIV-1 may increase its likelihood of encountering $CD4^+$ T cells. By failing to efficiently replicate in DCs, HIV-1 has the potential to avoid innate immune detection (Manel et al., 2010), and instead exploit DCs to rapidly and efficiently infect $CD4^+$ T cells through trans-enhancement. Such a model was recently supported by in vivo evidence for a contribution of trans-infection to retroviral spread in humanized mice (Sewald et al., 2015). Our genetic approach is a first step toward a better understanding of the molecular and cell biological aspects of HIV-1 transmission between DCs and T lymphocytes, which is needed to evaluate the importance of this process in animal models and, eventually, in infected

individuals. The genes identified in this study may thus serve as targets for limiting early HIV-1 transfer and propagation.

EXPERIMENTAL PROCEDURES

Transduction and shRNA screen

Blood monocytes were plated at 1 x 10^5 cells per well in 100 μl of medium with cytokines (hGM-CSF and hIL-4) and were transduced with 50 μl of SIVmac VLP/Vpx (Mangeot et al., 2002) in the presence of 5 μg/ml polybrene and 50 μl (10^7 i.u/ml) viral supernatant containing each shRNA from a human vesicular and membrane trafficking library (Broad institute (SIGMA)(Moffat et al., 2006)). Approximately 50,000 transduced MDDCs were recovered per well after 4 days of differentiation and were used for transfer experiments in co-cultures with autologous T cells and X4-HIV-1 GFP. See also Supplemental experimental procedures.

Trans-enhancement and flow cytometry analysis

After four days of stimulation with hGM-CSF (50ng/ml) and hIL-4 (10ng/ml), 50,000 MDDCs (1 million/ml) were mixed with 50,000 (1 million/ml) autologous $CD4^+$ T cells (activated for 4 days in the presence of phytohemagglutinin A (PHA-L 2 ug/ml) + IL-2 (10 IU/ml)) and 150 μl X4-tropic HIV-1 encoding GFP (50 ng $p24^{GAG}$, quantified by ELISA) per well in 96-well round bottom plates. Media was replaced after 24 h and GFP expression in T cells analyzed by flow cytometry another 24 h later. For flow cytometry analysis, cells were stained with anti-CD3 A700 (for T cells), anti-DC-SIGN PE (for MDDCs) and DAPI for live/dead gating. CountBright Absolute Counting Beads (Life Technologies) were used in each sample to assess changes in cell number. In some case, BD cytofix/cytoperm buffer and fixation protocol was used to detect intracellular P24 staining in both MDDCs and T cells during transfer and/or capture experiments.

Confocal microscopy

Microscopy was performed on a Zeiss 710 confocal with 405, 488, 543, and 633 nm lasers, a 63X N.A. 1.40 lens, and the pinhole set to 1 Airy unit as defined by Zeiss. Sequential scanning was used to assure no spillover of channels. Z series were taken at intervals of 400 nm.

Electron Microscopy

Cells were fixed in 0.1M sodium cacodylate buffer (pH 7.2), containing 2.5% glutaraldehyde and 2% paraformaldehyde for 2 hours and post-fixed with 1% osmium tetroxide for 1.5 hours at room temperature, then processed in a standard manner and embedded in EMbed 812 (Electron Microscopy Sciences, Hatfield, PA). Ultrathin sections (60 nm) were mounted on 200 mesh thin bar copper grids, stained with uranyl acetate and lead citrate, examined using Philips CM-12 electron microscope (FEI; Eindhoven, The Netherlands) and photographed with a Gatan (4k x 2.7k) digital camera (Gatan, Inc., Pleasanton, CA).

HIV-1 and dextran capture experiments

Four days after transduction with shRNAs, MDDCs were mixed with X4-HIV-GFP using the same conditions as with trans-infection experiments but without T cells. After 4 h co-culture, MDDCs were washed in cold PBS to remove unbound HIV-1 and RNA was extracted. After reverse transcription, the amount of HIV-1 RNA was detected by quantitative RT-PCR with primers for GFP (encoded inside the HIV genome) and normalized to GAPDH. For dextran capture experiments, MDDCs were loaded with 100μg/ml of dextran molecules of various size, for 30 min, washed extensively with cold PBS, and analyzed by flow cytometry.

Statistics

Unless otherwise specified, statistical analyses were done using The Holm-Sidak multiple comparison test following one way anova (NS; non significant; * $p<0.05$; ** $p<0.01$; *** $p<0.001$; **** $p<0.0001$). For most experiments, two different human blood donors were used and the average of triplicates and standard deviation was calculated for each blood donor.

Supplementary Material

Refer to Web version on PubMed Central for supplementary material.

Acknowledgments

We thank Nir Hacohen, David Root and Derya Unutmaz for help with the shRNA screen library design and generation; the NYULMC OCS Microscopy Core for the service provided for light and electron microscopy; the New York Structural Biology Center; Wendy Lin for technical help; Jarrod Johnson, Nicolas Manel, Sebastian Amigorena and Philippe Benaroche for their critical advice. This work was supported by fellowships from EMBO, the Cancer Research Institute and the Philippe Foundation (M.M.M), by the Howard Hughes Medical Institute (D.R.L.), the Helen and Martin Kimmel Center for Biology and Medicine (D.R.L.), NIH grant R21AI084633 (D.R.L.) and NCRR S10 RR023704-01A1.

References

Banchereau J, Briere F, Caux C, Davoust J, Lebecque S, Liu YJ, Pulendran B, Palucka K. Immunobiology of dendritic cells. Annual review of immunology. 2000; 18:767–811.

Bassani S, Cingolani LA, Valnegri P, Folci A, Zapata J, Gianfelice A, Sala C, Goda Y, Passafaro M. The X-linked intellectual disability protein TSPAN7 regulates excitatory synapse development and AMPAR trafficking. Neuron. 2012; 73:1143–1158. [PubMed: 22445342]

Berditchevski F. Complexes of tetraspanins with integrins: more than meets the eye. Journal of cell science. 2001; 114:4143–4151. [PubMed: 11739647]

Bergert M, Chandradoss SD, Desai RA, Paluch E. Cell mechanics control rapid transitions between blebs and lamellipodia during migration. Proceedings of the National Academy of Sciences of the United States of America. 2012; 109:14434–14439. [PubMed: 22786929]

Boettner DR, Chi RJ, Lemmon SK. Lessons from yeast for clathrin-mediated endocytosis. Nature cell biology. 2012; 14:2–10. [PubMed: 22193158]

Boggiano C, Manel N, Littman DR. Dendritic cell-mediated trans- enhancement of human immunodeficiency virus type 1 infectivity is independent of DC-SIGN. Journal of virology. 2007; 81:2519–2523. [PubMed: 17182696]

Cameron PU, Freudenthal PS, Barker JM, Gezelter S, Inaba K, Steinman RM. Dendritic cells exposed to human immunodeficiency virus type-1 transmit a vigorous cytopathic infection to CD4+ T cells. Science. 1992; 257:383–387. [PubMed: 1352913]

Casalou C, Seixas C, Portelinha A, Pintado P, Barros M, Ramalho JS, Lopes SS, Barral DC. Arl13b and the non-muscle myosin heavy chain IIA are required for circular dorsal ruffle formation and cell migration. Journal of cell science. 2014; 127:2709–2722. [PubMed: 24777479]

Cavrois M, Neidleman J, Greene WC. The achilles heel of the trojan horse model of HIV-1 trans-infection. PLoS pathogens. 2008; 4:e1000051. [PubMed: 18584030]

Cavrois M, Neidleman J, Kreisberg JF, Greene WC. In vitro derived dendritic cells trans-infect CD4 T cells primarily with surface-bound HIV-1 virions. PLoS pathogens. 2007; 3:e4. [PubMed: 17238285]

Charrin S, Jouannet S, Boucheix C, Rubinstein E. Tetraspanins at a glance. Journal of cell science. 2014; 127:3641–3648. [PubMed: 25128561]

Do T, Murphy G, Earl LA, Del Prete GQ, Grandinetti G, Li GH, Estes JD, Rao P, Trubey CM, Thomas J, et al. Three-dimensional imaging of HIV-1 virological synapses reveals membrane architectures involved in virus transmission. Journal of virology. 2014; 88:10327–10339. [PubMed: 24965444]

Doherty GJ, McMahon HT. Mechanisms of endocytosis. Annual review of biochemistry. 2009; 78:857–902.

Ferguson SM, De Camilli P. Dynamin, a membrane-remodelling GTPase. Nature reviews Molecular cell biology. 2012; 13:75–88. [PubMed: 22233676]

Gao D, Wu J, Wu YT, Du F, Aroh C, Yan N, Sun L, Chen ZJ. Cyclic GMP-AMP synthase is an innate immune sensor of HIV and other retroviruses. Science. 2013; 341:903–906. [PubMed: 23929945]

Garcia E, Pion M, Pelchen-Matthews A, Collinson L, Arrighi JF, Blot G, Leuba F, Escola JM, Demaurex N, Marsh M, et al. HIV-1 trafficking to the dendritic cell-T-cell infectious synapse uses a pathway of tetraspanin sorting to the immunological synapse. Traffic. 2005; 6:488–501. [PubMed: 15882445]

Gauthier NC, Masters TA, Sheetz MP. Mechanical feedback between membrane tension and dynamics. Trends in cell biology. 2012; 22:527–535. [PubMed: 22921414]

Geijtenbeek TB, Kwon DS, Torensma R, van Vliet SJ, van Duijnhoven GC, Middel J, Cornelissen IL, Nottet HS, KewalRamani VN, Littman DR, et al. DC-SIGN, a dendritic cell-specific HIV-1-binding protein that enhances trans-infection of T cells. Cell. 2000; 100:587–597. [PubMed: 10721995]

Glebov OO, Bright NA, Nichols BJ. Flotillin-1 defines a clathrin-independent endocytic pathway in mammalian cells. Nature cell biology. 2006; 8:46–54. [PubMed: 16341206]

Goley ED, Welch MD. The ARP2/3 complex: an actin nucleator comes of age. Nature reviews Molecular cell biology. 2006; 7:713–726. [PubMed: 16990851]

Gu C, Yaddanapudi S, Weins A, Osborn T, Reiser J, Pollak M, Hartwig J, Sever S. Direct dynamin-actin interactions regulate the actin cytoskeleton. The EMBO journal. 2010; 29:3593–3606. [PubMed: 20935625]

Hetrick B, Han MS, Helgeson LA, Nolen BJ. Small molecules CK-666 and CK-869 inhibit actin-related protein 2/3 complex by blocking an activating conformational change. Chemistry & biology. 2013; 20:701–712. [PubMed: 23623350]

Hilpela P, Vartiainen MK, Lappalainen P. Regulation of the actin cytoskeleton by PI(4,5)P2 and PI(3,4,5)P3. Current topics in microbiology and immunology. 2004; 282:117–163. [PubMed: 14594216]

Hubner W, Chen P, Del Portillo A, Liu Y, Gordon RE, Chen BK. Sequence of human immunodeficiency virus type 1 (HIV-1) Gag localization and oligomerization monitored with live confocal imaging of a replication-competent, fluorescently tagged HIV-1. Journal of virology. 2007; 81:12596–12607. [PubMed: 17728233]

Ivanov AI. Pharmacological inhibition of endocytic pathways: is it specific enough to be useful? Methods in molecular biology. 2008; 440:15–33. [PubMed: 18369934]

Izquierdo-Useros N, Lorizate M, Puertas MC, Rodriguez-Plata MT, Zangger N, Erikson E, Pino M, Erkizia I, Glass B, Clotet B, et al. Siglec-1 is a novel dendritic cell receptor that mediates HIV-1 trans-infection through recognition of viral membrane gangliosides. PLoS biology. 2012; 10:e1001448. [PubMed: 23271952]

Kaur S, Fielding AB, Gassner G, Carter NJ, Royle SJ. An unmet actin requirement explains the mitotic inhibition of clathrin-mediated endocytosis. eLife. 2014; 3:e00829. [PubMed: 24550251]

Kwon DS, Gregorio G, Bitton N, Hendrickson WA, Littman DR. DC-SIGN-mediated internalization of HIV is required for trans-enhancement of T cell infection. Immunity. 2002; 16:135–144. [PubMed: 11825572]

Laguette N, Sobhian B, Casartelli N, Ringeard M, Chable-Bessia C, Segeral E, Yatim A, Emiliani S, Schwartz O, Benkirane M. SAMHD1 is the dendritic- and myeloid-cell-specific HIV-1 restriction factor counteracted by Vpx. Nature. 2011; 474:654–657. [PubMed: 21613998]

Lahaye X, Satoh T, Gentili M, Cerboni S, Conrad C, Hurbain I, El Marjou A, Lacabaratz C, Lelievre JD, Manel N. The Capsids of HIV-1 and HIV-2 Determine Immune Detection of the Viral cDNA by the Innate Sensor cGAS in Dendritic Cells. Immunity. 2013

Lee E, De Camilli P. Dynamin at actin tails. Proceedings of the National Academy of Sciences of the United States of America. 2002; 99:161–166. [PubMed: 11782545]

Manel N, Hogstad B, Wang Y, Levy DE, Unutmaz D, Littman DR. A cryptic sensor for HIV-1 activates antiviral innate immunity in dendritic cells. Nature. 2010; 467:214–217. [PubMed: 20829794]

Mangeot PE, Duperrier K, Negre D, Boson B, Rigal D, Cosset FL, Darlix JL. High levels of transduction of human dendritic cells with optimized SIV vectors. Molecular therapy : the journal of the American Society of Gene Therapy. 2002; 5:283–290. [PubMed: 11863418]

Martin AC, Welch MD, Drubin DG. Arp2/3 ATP hydrolysis-catalysed branch dissociation is critical for endocytic force generation. Nature cell biology. 2006; 8:826–833. [PubMed: 16862144]

McDonald D, Wu L, Bohks SM, KewalRamani VN, Unutmaz D, Hope TJ. Recruitment of HIV and its receptors to dendritic cell-T cell junctions. Science. 2003; 300:1295–1297. [PubMed: 12730499]

Menon M, Askinazi OL, Schafer DA. Dynamin2 organizes lamellipodial actin networks to orchestrate lamellar actomyosin. PloS one. 2014; 9:e94330. [PubMed: 24710573]

Mercer J, Helenius A. Vaccinia virus uses macropinocytosis and apoptotic mimicry to enter host cells. Science. 2008; 320:531–535. [PubMed: 18436786]

Moffat J, Grueneberg DA, Yang X, Kim SY, Kloepfer AM, Hinkle G, Piqani B, Eisenhaure TM, Luo B, Grenier JK, et al. A lentiviral RNAi library for human and mouse genes applied to an arrayed viral high-content screen. Cell. 2006; 124:1283–1298. [PubMed: 16564017]

Nikolic DS, Lehmann M, Felts R, Garcia E, Blanchet FP, Subramaniam S, Piguet V. HIV-1 activates Cdc42 and induces membrane extensions in immature dendritic cells to facilitate cell-to-cell virus propagation. Blood. 2011; 118:4841–4852. [PubMed: 21562048]

Orth JD, Krueger EW, Cao H, McNiven MA. The large GTPase dynamin regulates actin comet formation and movement in living cells. Proceedings of the National Academy of Sciences of the United States of America. 2002; 99:167–172. [PubMed: 11782546]

Ridley AJ. Life at the leading edge. Cell. 2011; 145:1012–1022. [PubMed: 21703446]

Rocca DL, Martin S, Jenkins EL, Hanley JG. Inhibition of Arp2/3-mediated actin polymerization by PICK1 regulates neuronal morphology and AMPA receptor endocytosis. Nature cell biology. 2008; 10:259–271. [PubMed: 18297063]

Rohatgi R, Ma L, Miki H, Lopez M, Kirchhausen T, Takenawa T, Kirschner MW. The interaction between N-WASP and the Arp2/3 complex links Cdc42-dependent signals to actin assembly. Cell. 1999; 97:221–231. [PubMed: 10219243]

Sarkar K, Kruhlak MJ, Erlandsen SL, Shaw S. Selective inhibition by rottlerin of macropinocytosis in monocyte-derived dendritic cells. Immunology. 2005; 116:513–524. [PubMed: 16313365]

Sewald X, Ladinsky MS, Uchil PD, Beloor J, Pi R, Herrmann C, Motamedi N, Murooka TT, Brehm MA, Greiner DL, et al. Retroviruses use CD169-mediated trans-infection of permissive lymphocytes to establish infection. Science. 2015

Straight AF, Cheung A, Limouze J, Chen I, Westwood NJ, Sellers JR, Mitchison TJ. Dissecting temporal and spatial control of cytokinesis with a myosin II Inhibitor. Science. 2003; 299:1743–1747. [PubMed: 12637748]

Wang JTH, Teasdale RD, Liebl D. Macropinosome quantitation assay. MethodsX. 2014; 1:36–41. [PubMed: 26150932]

Wu L, KewalRamani VN. Dendritic-cell interactions with HIV: infection and viral dissemination. Nature reviews Immunology. 2006; 6:859–868.

Yamada H, Abe T, Li SA, Masuoka Y, Isoda M, Watanabe M, Nasu Y, Kumon H, Asai A, Takei K. Dynasore, a dynamin inhibitor, suppresses lamellipodia formation and cancer cell invasion by destabilizing actin filaments. Biochemical and biophysical research communications. 2009; 390:1142–1148. [PubMed: 19857461]

Yang Q, Zhang XF, Pollard TD, Forscher P. Arp2/3 complex-dependent actin networks constrain myosin II function in driving retrograde actin flow. The Journal of cell biology. 2012; 197:939–956. [PubMed: 22711700]

Yauch RL, Hemler ME. Specific interactions among transmembrane 4 superfamily (TM4SF) proteins and phosphoinositide 4-kinase. The Biochemical journal. 2000; 351(Pt 3):629–637. [PubMed: 11042117]

Yu HJ, Reuter MA, McDonald D. HIV traffics through a specialized, surface-accessible intracellular compartment during trans-infection of T cells by mature dendritic cells. PLoS pathogens. 2008; 4:e1000134. [PubMed: 18725936]

Zemni R, Bienvenu T, Vinet MC, Sefiani A, Carrie A, Billuart P, McDonell N, Couvert P, Francis F, Chafey P, et al. A new gene involved in X-linked mental retardation identified by analysis of an X; 2 balanced translocation. Nature genetics. 2000; 24:167–170. [PubMed: 10655063]

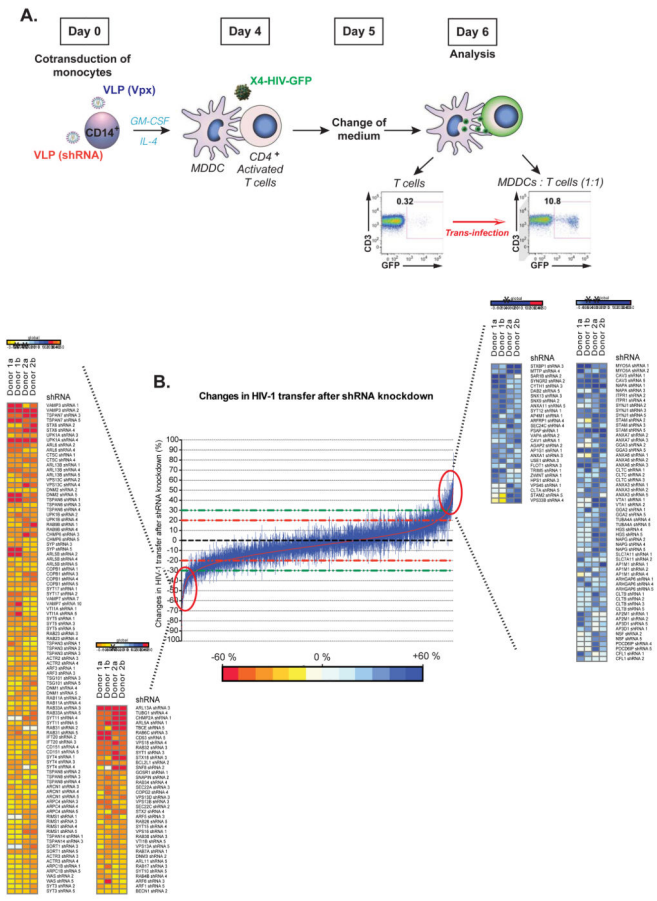

Figure 1. Strategy and aggregate results for the trans-enhancement shRNA screen

A. Schematic representation of the strategy used to perform the shRNA screen. **B.** Results of the shRNA screen, displayed as the percent change in proportion of infected T cells relative to the proportion observed with scrambled control shRNAs. For each shRNA, the average of two biological replicates is displayed as a red dot and the standard deviation is depicted by a blue line. The dashed red line symbolizes an arbitrary cut off of +/− 20% for non-specific variation in HIV-1 transfer, and the green dashed line (+/− 30%) demarcates hits. For each gene the sum of the effect of all shRNAs on trans-enhancement was calculated and the average effect per shRNA was used as a ranking score for the hits (Table S1). Potential hits are shown in heat maps depending on the presence of at least 2 shRNAs (**) or one shRNA (*) among the hits. See also Figure S1 and Table S1.

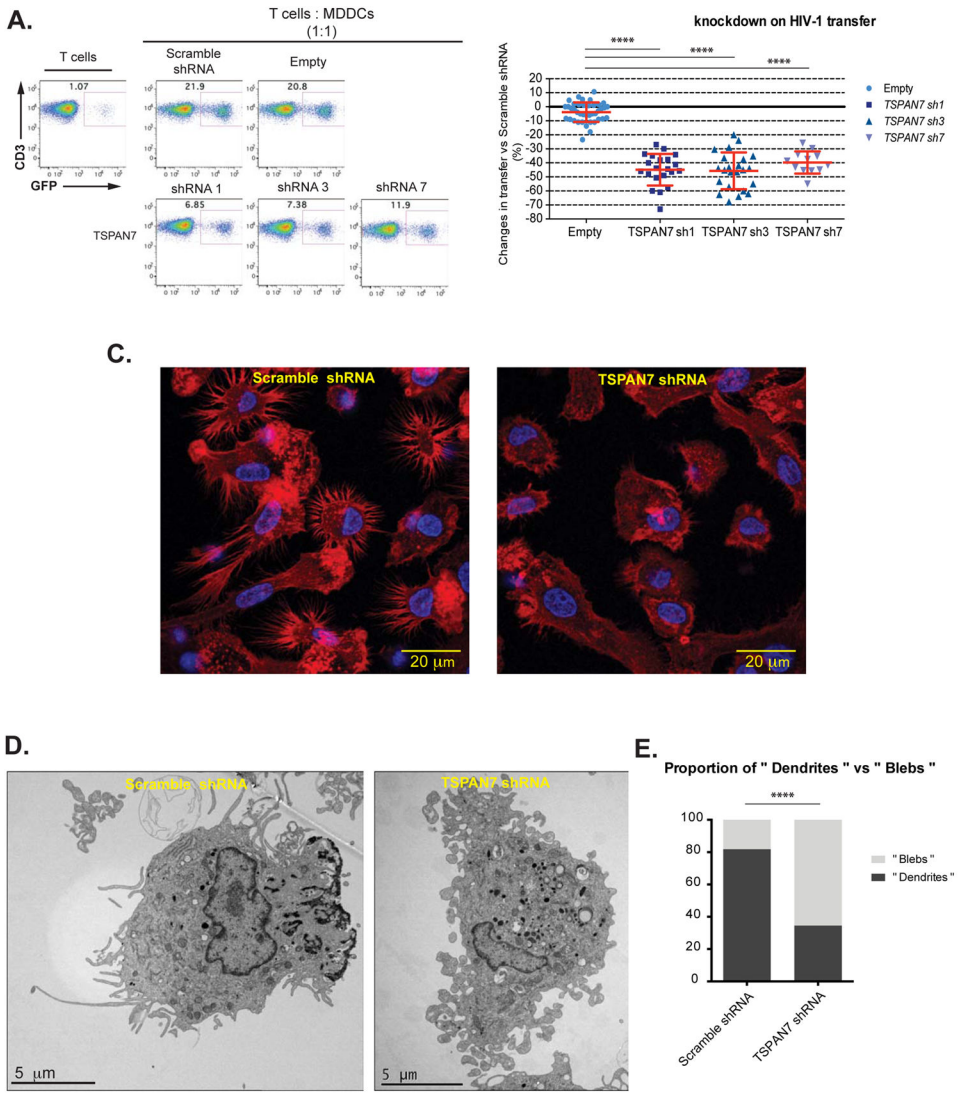

Figure 2. TSPAN7 requirement for HIV-1 transfer and dendrite formation

A. Representative trans-enhancement results following knockdown in MDDCs of TSPAN7 with 3 different shRNAs, as compared to control vectors. **B.** Aggregate results of effect of TSPAN7 knockdown on trans-enhancement using MDDCs and T cells from multiple human blood donors. The amount of HIV-1 transfer is displayed as a percentage of change compared to the proportion of GFP^+ T cells obtained after co-culture with MDDCs transduced with a scrambled shRNA. **C.** Confocal microscopy images of MDDCs stained for filamentous actin with phalloidin (red) and for nuclei with Dapi (blue), 4 days after transduction with either scrambled or TSPAN7 shRNAs. One Z-stack of 400nm is displayed. **D.** Electron microscopic images of representative MDDCs, 4 days after transduction with control or TSPAN7 shRNAs. **E.** Quantification of the proportion of MDDCs with “dendrites” versus “blebs” as shown in panel D. N=70 cells for scrambled shRNA and N=150 cells for TSPAN7 shRNA. Statistical differences were calculated based on two-tailed Fisher’s exact test. See also Figure S2 and Movie S1.

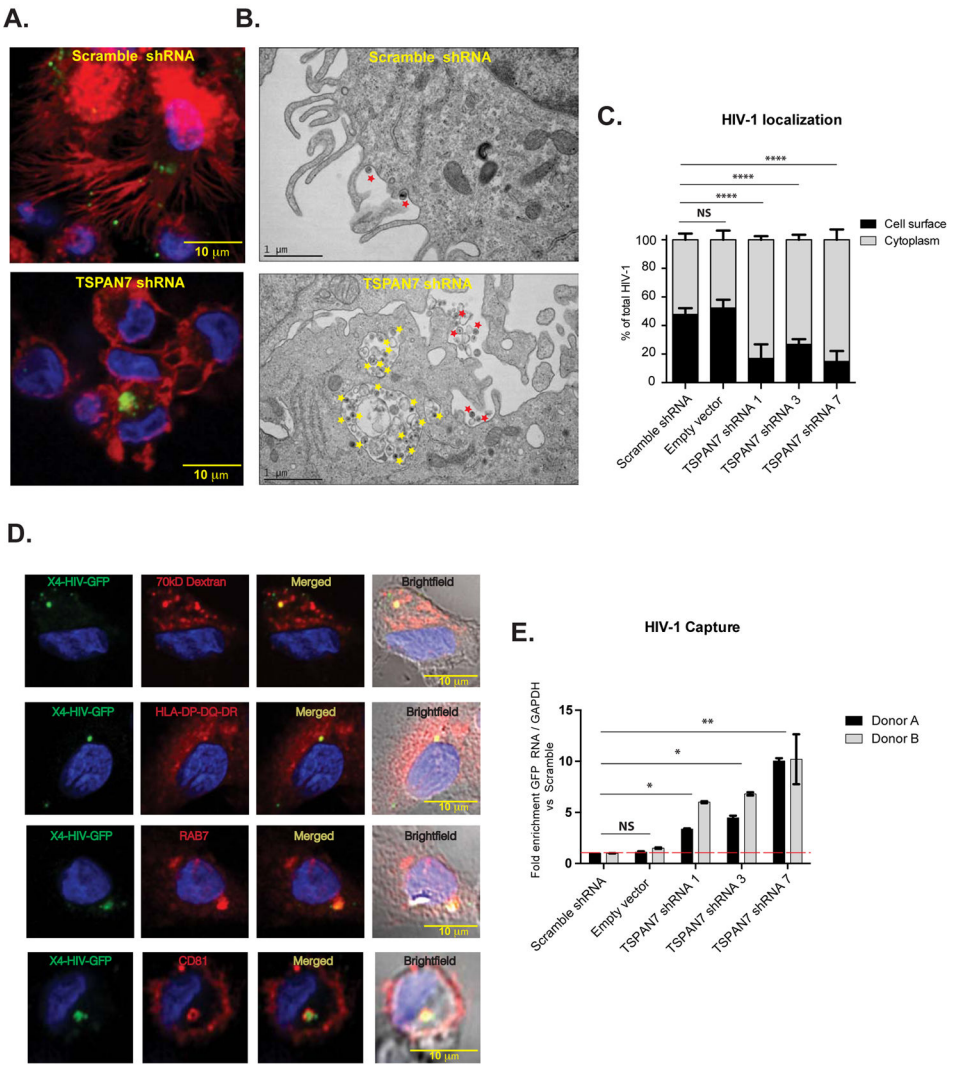

Figure 3. Redistribution of HIV-1 from dendrites to macropinosome-like structures upon TSPAN7 knockdown

A. Confocal microscopy analysis of MDDCs transduced with either scrambled or TSPAN7 shRNAs and co-cultured for 24 h with autologous activated T cells and HIV-iGAG-GFP. Staining is for filamentous actin (phalloidin, red) and nuclear DNA (DAPI, blue). Each image represents a Z-stack of 400nm. **B.** Electron microscopy images of dendritic cells co-cultured as in A. Zoomed segments of the plasma membrane are displayed to show the presence of HIV-1 either at the surface (red stars) or concentrated inside macropinosome-like structures (yellow stars). **C.** Numbers of HIV-1 particles associated with dendrites/cell surface versus cytosolic compartments, assessed at 4 h co-culture for approximately 200 cells with 15 Z-stacks of 400nm each. Statistical differences were calculated based on two-tailed Fisher's exact test. **D.** MDDCs transduced with TSPAN7 shRNA were cultured with X4-HIV-iGAG-GFP and 70kD dextran or X4HIV-iGAG-GFP alone for 4 h and immunostained for the indicated markers. One representative image is shown for each cellular marker tested. DAPI stains the nuclei, GFP represents HIV-1, and cellular markers are displayed in red. **E.** Quantification of HIV-1 capture by MDDCs, 4 h after co-culture.

The amount of HIV-1 RNA associated with the cells was measured by reverse transcription/quantitative real time PCR with primers specific for GFP (encoded within the HIV genome) and normalized to GAPDH primers. Each condition was compared to the amount of HIV-1 RNA after transduction with scrambled shRNA (arbitrarily set at 1 (red line)).

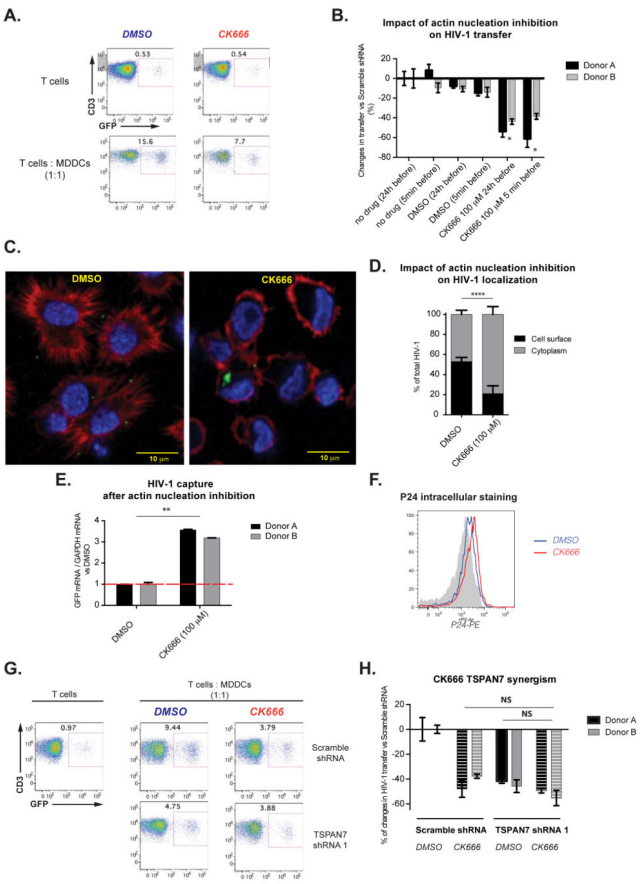

Figure 4. Inhibition of actin nucleation complex ARP2/3 mimics the TSPAN7 knockdown phenotype

A. Trans-enhancement following treatment of MDDCs with the ARP2/3 inhibitor CK666 (100 μM), added 5 min before co-culture with autologous activated T cells and X4-HIV-GFP. **B.** Effect on transfer of CK666 compared to DMSO, showing average of triplicates for two independent blood donors. **C.** Confocal microscopy images of MDDCs treated with DMSO or CK666 (100 μM) 5 min before addition of HIV-1. Analysis was at 24 h after the start of co-culture, Actin filaments are stained in red (phalloidin stain), HIV-igag-GFP in green, and nuclei in blue (DAPI). **D.** Quantification of HIV-1 localization at 4 h of treatment with DMSO or CK666. For each condition, approximately 200 cells with 15 Z-stacks per cell, coming from two different donors in two independent experiments, were analyzed. Statistical differences were calculated based on two-tailed Fisher's exact test. **E.** Quantification of HIV-1 capture by MDDCs at 4 h following treatment with either DMSO or CK666. Data are normalized to GAPDH RNA and compared to the amount of HIV-1 captured after DMSO treatment (arbitrarily set up to 1 (Red dashed line)). Statistical differences were calculated based on two-tailed Fisher's exact test. **F.** Intracellular staining for p24, in MDDCs incubated with HIV-1 in the presence of DMSO or CK666 for 4 h. Gray, isotype control; blue, DMSO treatment; red, CK666 treatment. **G.** Flow cytometry analysis of $CD4^+$ T cells, after coculture with MDDCs transduced with scrambled or TSPAN7 shRNAs and treated with DMSO or CK666 (100 μM) before co-culture with T

cells and HIV-1. **H.** Percent reduction of HIV-1 transfer following ARP2/3 inhibition and TSPAN7 knockdown in MDDCs. See also Figure S3.

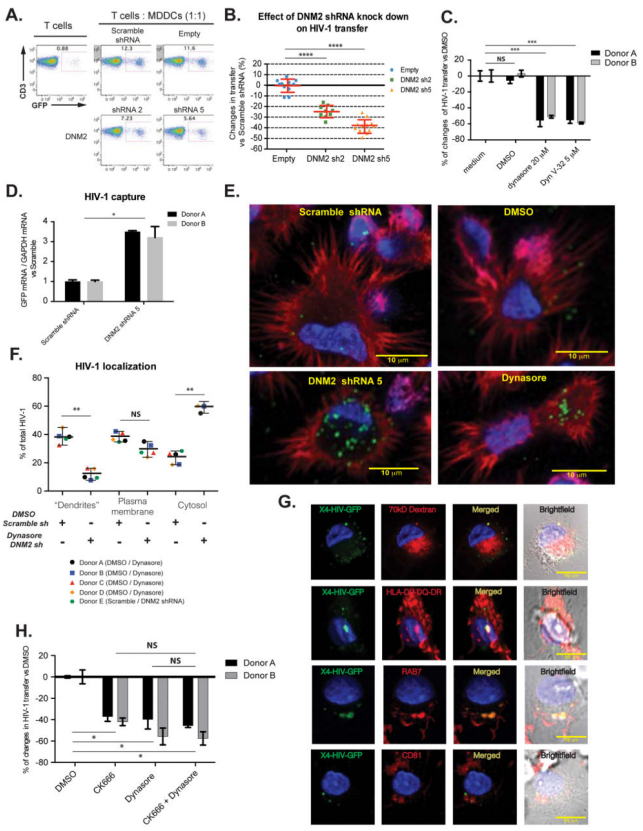

Figure 5. Inhibition of DNM2 function in MDDCs reduces HIV-1 trans-infection and concentrates viral particles in macropinosome-like vesicles

A. Representative trans-enhancement results following knockdown in MDDCs of DNM2 (lower panels) as compared to control vectors (upper panels). **B**. Aggregate results of effect of DNM2 knockdown on trans-enhancement using MDDCs and T cells from multiple human blood donors. **C**. Effect of dynamin inhibitors on HIV-1 trans-enhancement. MDDCs were treated with inhibitors of DNM2 function (dynasore, 20 μM, or Dyn V-32, 5 μM) or with DMSO one hour before co-culture with T cells and HIV-GFP. Results are displayed as percent change in HIV transfer compared to DMSO treatment. **D**. Quantification of HIV-1 capture by MDDCs following transduction with DNM2 or scrambled shRNAs. The two-tailed exact t-test was used to determine statistical differences. **E**. Confocal microscopy analysis of HIV-1 localization, 4 h after incubation with MDDCs transduced with scrambled or DNM2 shRNA (left panels) or treated with DMSO or dynasore (right panel). Red, phalloidin staining; green, HIV-iGAG-GFP; blue, nuclear DAPI staining. **F**. Quantification of HIV-1 localization based on confocal analysis as shown in panel E. For each donor, approximately 200 cells, with 15 Z-stacks per cell, were analyzed. **G**. MDDCs transduced with DNM2 shRNA were cultured with X4-HIV-iGAG-GFP and 70kD dextran or X4HIV-iGAG-GFP alone for 4 h and immunostained for the indicated markers. DAPI stains the nuclei, GFP represents HIV-1, and cellular markers are displayed in red. **H.** Effect on HIV-1 transfer of MDDC treatment with CK666 (5 min before co-culture), dynasore (1 h before co-culture), or the combination of both drugs. Results are percent change compared to the

baseline proportion of infected T cells when MDDCs were treated with DMSO. See also Figure S4 and S5.

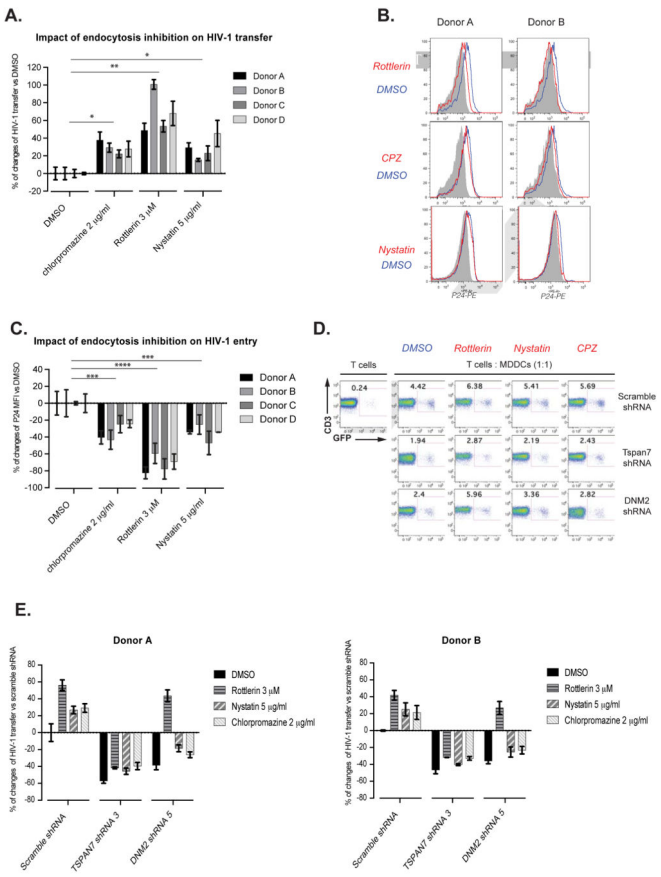

Figure 6. Rescue of HIV-1 transfer by inhibition of macropinocytosis in MDDCs

A. Influence on trans-enhancement by inhibitors of different endocytic pathways. MDDCs were treated with each drug for 2 h, washed, and co-cultured with HIV-GFP and autologous activated T cells. Results are displayed as percent change in HIV-1 infected T cells, compared to baseline of MDDCs treated with DMSO. **B.** HIV-1 capture by MDDCs, detected by flow cytometry after p24 staining, following inhibition of different endocytic pathways (red line) as compared to DMSO treatment (blue line). Gray: isotype control. **C.** Mean fluorescence intensity (MFI) for p24 staining in experiments represented in panel B. **D.** Effect on trans-enhancement of endocytosis pathway inhibitors incubated, 2 hours prior to co-culture with virus and T cells, with MDDCs previously transduced with shRNAs targeting TSPAN7 or DNM2. **E.** Percent change in HIV-1 transfer when MDDCs transduced with scrambled, TSPAN7 or DNM2 shRNAs, were treated with endocytosis inhibitors or DMSO, as in panel D. Two independent experiments performed with different blood donors are shown in the left and right histograms. See also Figure S6.

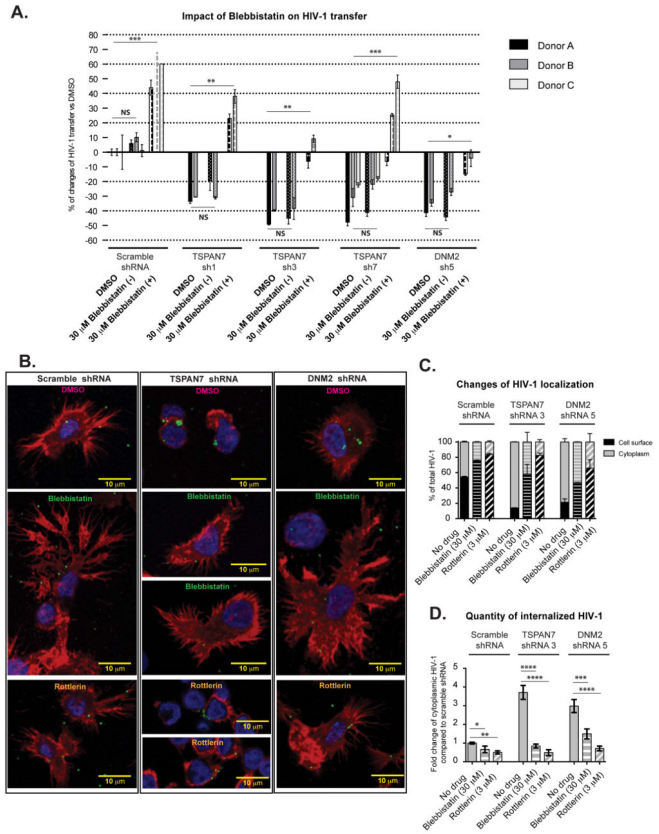

Figure 7. Inhibition of actomyosin contraction enhances HIV-1 transfer and rescues effects of TSPAN7 and DNM2 knockdown

A. Effect of blebbistatin treatment on HIV-1 transfer from MDDCs to CD4$^+$ T cells. MDDCs were treated for 2 h with 30 μM of an active or inactive version (enantiomers) of blebbistatin, washed, and co-cultured with X4-HIV-GFP and autologous activated T cells. Results are displayed as percent change in HIV-1 transfer compared to baseline of MDDC knockdown with scramble shRNA. **B.** Confocal microscopy analysis of blebbistatin and rottlerin effects on HIV-1 localization and dendrite formation in MDDCs transduced with scrambled (left panel), TSPAN7 (middle panel) or DNM2 (right panel) shRNAs. 30 μM of blebbistatin or 3 μM of rottlerin were applied to MDDCs for 2 h, washed away, and cells were imaged 24 hours after coculture with HIV-1 and T cells. Red, phalloidin staining; green, HIV-iGAG-GFP; blue, nuclear DAPI staining. **C.** Quantification of HIV-1 localization based on confocal analysis as shown in B. For each donor, approximately 50 cells, with 15 Z-stacks per cell, were analyzed. Percentage of total HIV-1 distribution is shown. **D.** Results of the confocal experiment in B are displayed as fold change of internalized HIV-1 and compared and normalized to the amount of HIV-1 internalized following knockdown with scramble shRNA. See also Figure S7.